

Single-layer graphene cathodes for organic photovoltaics

Marshall Cox, Alon Gorodetsky, Bumjung Kim, Keun Soo Kim, Zhang Jia et al.

Citation: *Appl. Phys. Lett.* **98**, 123303 (2011); doi: 10.1063/1.3569601

View online: <http://dx.doi.org/10.1063/1.3569601>

View Table of Contents: <http://apl.aip.org/resource/1/APPLAB/v98/i12>

Published by the [American Institute of Physics](#).

Related Articles

Analysis of a device model for organic pseudo-bilayer solar cells
J. Appl. Phys. **112**, 084511 (2012)

Addition of regiorandom poly(3-hexylthiophene) to solution processed poly(3-hexylthiophene):[6,6]-phenyl-C61-butyric acid methyl ester graded bilayers to tune the vertical concentration gradient
APL: Org. Electron. Photonics **5**, 235 (2012)

Addition of regiorandom poly(3-hexylthiophene) to solution processed poly(3-hexylthiophene):[6,6]-phenyl-C61-butyric acid methyl ester graded bilayers to tune the vertical concentration gradient
Appl. Phys. Lett. **101**, 173301 (2012)

Tunable open-circuit voltage in ternary organic solar cells
Appl. Phys. Lett. **101**, 163302 (2012)

Tunable open-circuit voltage in ternary organic solar cells
APL: Org. Electron. Photonics **5**, 233 (2012)

Additional information on *Appl. Phys. Lett.*

Journal Homepage: <http://apl.aip.org/>

Journal Information: http://apl.aip.org/about/about_the_journal

Top downloads: http://apl.aip.org/features/most_downloaded

Information for Authors: <http://apl.aip.org/authors>

ADVERTISEMENT

**Universal charged-particle detector
for interdisciplinary applications:**

- > Non-scanning Mass Spectrometry
- > Non-scanning Ion Mobility Spectrometry
- > Non-scanning Electron Spectroscopy
- > Direct microchannel plate readout
- > Thermal ion motion and mobility studies
- > Bio-molecular ion soft-landing profiling
- > Real-time beam current/shape tuning
- > Diagnostics tool for instrument design
- > Compact linear array for beam lines

Contact **OI Analytical**: +1-205-733-6900

The advertisement features a 3D perspective of a detector array. A rainbow-colored arrow points from left to right across the top of the array. The arrow is labeled with 'Thermal', 'hyper-thermal', and 'keV-energy ions'. Below the arrow, the text reads 'Atmospheric Pressure to Ultra High Vacuum'. The main product name 'IonCCD™' is prominently displayed in the center. To the right of the product name, it says 'for charged particles'. Below this, two key specifications are listed: '24µm spatial resolution (2136 pixels)' and '3ns temporal resolution (360fps)'. In the top right corner, the 'OI Analytical' logo is visible, consisting of the text 'OI Analytical' next to a stylized globe icon.

Single-layer graphene cathodes for organic photovoltaics

Marshall Cox,^{1,a)} Alon Gorodetsky,² Bumjung Kim,² Keun Soo Kim,³ Zhang Jia,¹ Philip Kim,³ Colin Nuckolls,² and Ioannis Kymissis¹

¹Department of Electrical Engineering, Columbia University–New York, New York 10027, USA

²Department of Chemistry, Columbia University–New York, New York 10027, USA

³Department of Physics, Columbia University–New York, New York 10027, USA

(Received 16 December 2010; accepted 2 March 2011; published online 23 March 2011)

A laminated single-layer graphene is demonstrated as a cathode for organic photovoltaic devices. The measured properties indicate that graphene offers two potential advantages over conventional photovoltaic electrode materials; work function matching via contact doping, and increased power conversion efficiency due to transparency. These findings indicate that flexible, light-weight all carbon solar cells can be constructed using graphene as the cathode material. © 2011 American Institute of Physics. [doi:10.1063/1.3569601]

Graphene, a two-dimensional crystalline form of carbon, was first isolated by Novoselov *et al.* in 2004.^{1,2} The high transparency,³ conductivity,^{4–8} flexibility,^{9–11} and elemental abundance of graphene indicate that it is an excellent replacement for transparent conducting oxide electrodes. Graphene¹¹ and graphene oxide^{12–14} have been previously considered as anode materials in organic photovoltaic devices (OPVs). Here, we describe OPV devices with single-layer chemical vapor deposition (CVD) grown graphene as a cathode.

While several studies have demonstrated that graphene can serve as an anode material, there is only a single study that has utilized graphene as a cathode material.¹⁵ In this work, multilayer graphene modified with a dipole layer served as the cathode in poly(3-hexylthiophene)/[6,6]-phenyl-C61-butyric acid methyl ester (P3HT/PCBM) OPVs; interestingly, a photoresponse was observed for devices from dipole layer treated graphene, but not for devices from bare graphene. To understand this effect, it is important to note that as a result of graphene's small density of states around the Dirac point, single-layer graphene exhibits a highly tunable work function that shifts when it contacts other materials.^{16–18} Furthermore, in PCBM:P3HT bulk heterojunctions, the P3HT segregates at electrode surfaces.¹⁹ Therefore, when bare graphene comes into contact with an electron donor (P3HT) charge transfer will “contact dope” the cathode or raise its work function. This effect would not be expected for graphene treated with a dipole layer.

To demonstrate the utility of contact doping, we fabricated OPVs with laminated graphene cathodes (the device architecture and corresponding band diagram are shown in Figs. 1(a) and 1(b)). Prepatterned indium–tin–oxide (ITO) substrates (Luminescence Technology Corporation) were solvent cleaned, exposed to UV-ozone (Jelight UVO cleaner) for 10 min, and coated with PEDOT (HC Starck) at 3000 rpm for 60 s. The samples were baked at 120 °C for 45 min and then transferred into a nitrogen glove box-coupled vacuum deposition system (Angstrom Engineering) for device fabrication. 40 nm of copper phthalocyanine (CuPC), 40 nm of C₆₀, and 10 nm of 1,3,5-tri(phenyl-2-benzimidazole)-

benzene (TPBi) (Refs. 20 and 21) were evaporated in succession to form the device stack.

To complete the devices, the electrodes were fabricated as follows. For the graphene devices, graphene was grown via CVD and transferred to a polydimethylsiloxane (PDMS, Sylgard 184) substrate as previously described.^{10,22–25} This graphene/PDMS “stamp” was used to laminate the graphene cathode, yielding an active area of 0.4 cm² [Figs. 1(c) and 1(d)]. For the aluminum control devices, 60 nm of Al was evaporated as a cathode, yielding an active area of 0.16 cm². *I-V* measurements were performed under AM 1.5 solar simulated illumination in a nitrogen environment and under various monochromatic (620 nm) LED intensities (using the Luminus Devices Phlat Light PT-120-R) in ambient.

Figure 2 shows typical *I-V* curves for graphene and Al devices (100 mW/cm²), which clearly indicate that these graphene cathode devices function as solar cells in the absence of chemical doping or work function matching. The graphene devices exhibit a power efficiency of 0.02% and the aluminum controls exhibit a power conversion efficiency of 0.41%. The open circuit voltage (*V*_{OC}) for both types of devices is approximately 0.45 V. This large efficiency dispar-

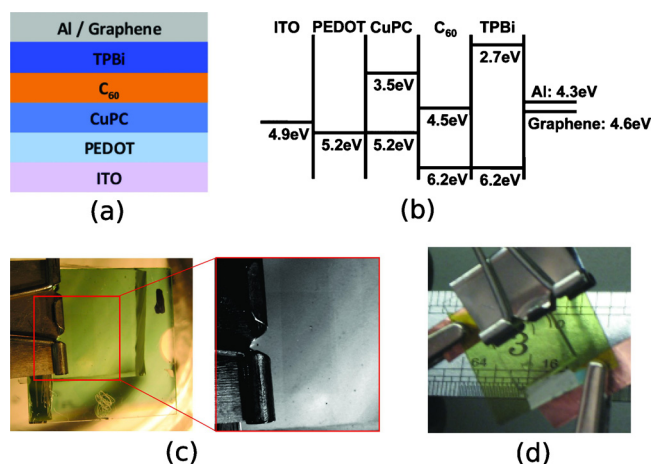


FIG. 1. (Color online) (a) Schematic illustration of the device architecture. (b) The HOMO and LUMO energy level diagram of the device with values equal to the energy below the vacuum level. (c) Image of a graphene device which shows the vertical ITO anode strip and the graphene cathode (graphene edges are indicated by arrows). (d) Image of a graphene device illustrating its high transparency.

^{a)}Electronic mail: mpc2139@columbia.edu.

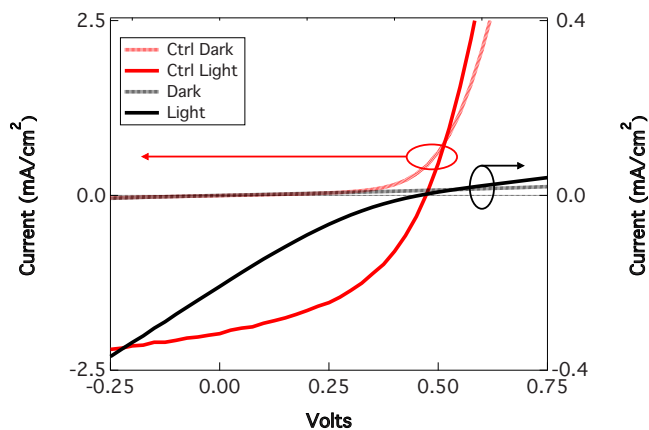


FIG. 2. (Color online) I - V characteristics for graphene and aluminum cathode devices under 100 mW/cm^2 solar simulated illumination.

ity in conjunction with similar V_{OC} 's indicates that parasitic series resistances dominate the characteristics of the graphene devices. To quantify the differences between aluminum and graphene cathode devices, both data sets were fit to the ideal diode equation. The fit yielded a series resistance of $700 \text{ } \Omega$ and a shunt resistance of $10 \text{ k}\Omega$ in the control devices versus a series resistance $10.5 \text{ k}\Omega$ and shunt resistance of $3.5 \text{ k}\Omega$ for the graphene cathode devices. The large parasitic resistances of the graphene devices directly induces lower efficiencies due to poor fill-factors under solar illumination. This observation is analogous to the series resistance/fill factor degradation found in few-layer graphene anode devices.^{12,14,26}

To minimize the influence of the parasitic series resistance we probed the devices under low-intensity monochromatic illumination (Fig. 3). At an incident power of 4.6 mW/cm^2 , the graphene device exhibits a power conversion efficiency of 0.22% and a V_{OC} of 0.38 V , while the aluminum cathode device exhibits a power conversion efficiency of 1.19% and a V_{OC} of 0.38 V . At an incident power of 6.6 mW/cm^2 , the graphene device exhibits a power conversion efficiency of 0.24% and a V_{OC} of 0.40 V , while the aluminum device exhibits a power conversion efficiency of 1.84% and a V_{OC} of 0.43 V . Given the 0.3 eV difference between the work functions of graphene and aluminum, the nearly identical V_{OC} values can only be the result of graphene undergoing contact doping and adjusting its work

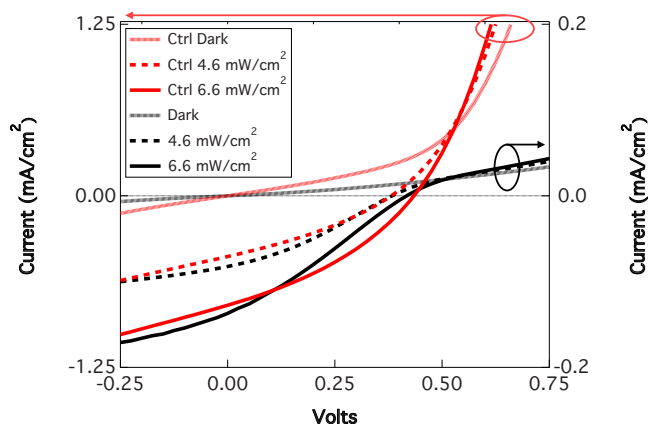


FIG. 3. (Color online) Graphene and aluminum control devices were analyzed under different illumination intensities to investigate fill factor and V_{OC} as a function of incident power.

function upon contact with a strong electron acceptor (TPBi).

The optical transparency of graphene also enabled us to compare device performance with both anode and cathode-side illumination [Fig. 1(d)]. The power conversion efficiency was 0.01% for anode-side solar illumination and 0.03% for cathode-side solar illumination. In addition, the power conversion efficiency was 0.24% for anode-side monochromatic illumination (6.57 mW/cm^2) and 0.41% for cathode-side monochromatic illumination (6.57 mW/cm^2). These differences in device performance were due to an increase in the short-circuit current density for cathode-side illumination. We attribute this difference to the strong absorbance of CuPC. Anode side illumination results in the majority of excitons being formed at the PEDOT/CuPC junction, which is not within an exciton diffusion length of the power producing CuPC/ C_{60} interface. Cathode side illumination results in the majority of excitons being produced at the energy producing CuPC/ C_{60} heterojunction. This leads to an increase in efficiency for cathode-side illumination relative to anode-side illumination.

We have demonstrated that single-layer graphene undergoes contact doping and can serve as cathodes in OPVs. The power conversion efficiencies of graphene devices were limited by their series resistance, indicating that the preparation of graphene samples with lower sheet resistances could improve device performance. The V_{OC} 's of our devices indicated that the work functions of graphene sheets shift when placed in contact with electron-donating material. This type of contact doping is a potentially valuable characteristic. The transparency of graphene also enabled us to demonstrate a simple strategy for doubling the efficiency of OPVs. The demonstration of a functioning graphene cathode device allows for the fabrication of all-graphene electrode devices. These findings favorably indicate the possibility of fabricating metal free, truly organic solar cells with graphene as a cathode and anode.

This material is based upon work supported as part of the Center for Re-Defining Photovoltaic Efficiency through Molecule Scale Control, an Energy Frontier Research Center funded by the U.S. Department of Energy, Office of Science, Office of Basic Energy Sciences under Award No. DE-SC0001085, and by the National Science Foundation under Award No. CHE-0936923.

¹K. S. Novoselov, A. K. Geim, S. V. Morozov, D. Jiang, Y. Zhang, S. V. Dubonos, I. V. Grigorieva, and A. A. Firsov, *Science* **306**, 666 (2004).

²K. S. Novoselov, D. Jiang, F. Schedin, T. J. Booth, V. V. Khotkevich, S. V. Morozov, and A. K. Geim, *Proc. Natl. Acad. Sci. U.S.A.* **102**, 10451 (2005).

³R. R. Nair, P. Blake, A. N. Grigorenko, K. S. Novoselov, T. J. Booth, T. Stauber, N. M. R. Peres, and A. K. Geim, *Science* **320**, 1308 (2008).

⁴Y. Zhang, Y.-W. Tan, H. L. Stormer, and P. Kim, *Nature (London)* **438**, 201 (2005).

⁵Y.-W. Tan, Y. Zhang, K. Bolotin, Y. Zhao, S. Adam, E. H. Hwang, S. Das Sarma, H. L. Stormer, and P. Kim, *Phys. Rev. Lett.* **99**, 246803 (2007).

⁶A. K. Geim and K. S. Novoselov, *Nature Mater.* **6**, 183 (2007).

⁷R. R. Nair, T. J. Booth, D. J. Fred Schedin, L. A. Ponomarenko, S. V. Morozov, H. F. Gleason, E. W. Hill, A. K. Geim, P. Blake, P. D. Brimicombe, and K. S. Novoselov, *ACS Nano* **8**, 1281 (2008).

⁸M. C. Lemme, T. J. Echtermeyer, M. Baus, B. N. Szafrank, J. Bolten, M. Schmidt, T. Wahlbrink, and H. Kurz, *Solid-State Electron.* **52**, 514 (2008).

⁹C. Lee, X. Wei, J. W. Keysar, and J. Hone, *Science* **321**, 385 (2008).

¹⁰K. S. Kim, Y. Zhao, H. Jang, S. Y. Lee, J. M. Kim, K. S. Kim, J.-H. Ahn, P. Kim, J.-Y. Choi, and B. H. Keun, *Nature (London)* **457**, 706 (2009).

¹¹L. G. De Arco, Y. Zhang, C. W. Schlenker, K. Ryu, M. E. Thompson, and

- C. Zhou, *ACS Nano* **4**, 2865 (2010).
- ¹²S. Miller, C.-W. Chen, W.-F. Su, G. Eda, Y.-Y. Lin, and M. Chhowalla, *Appl. Phys. Lett.* **92**, 163501 (2008).
- ¹³X. Wang, L. Zhi, and K. Müllen., *ACS Nano* **8**, 323 (2008).
- ¹⁴Z. Bao, Z. Liu, Y. Chen, J. Wu, H. A. Becerril, and P. Peumans, *Appl. Phys. Lett.* **92**, 263302 (2008).
- ¹⁵S.-H. Oh, S. L. Tae-Soo Kim, G. Wang, M. Choe, W. Park, J. Yoon, D.-Y. Kim, Y. H. Kahng, T. Lee, G. Jo, and S.-I. Na, *Appl. Phys. Lett.* **97**, 213301 (2010).
- ¹⁶S. Ryu, L. E. Brus, K. S. Kim, P. Kim, Y.-J. Yu, and Y. Zhao, *ACS Nano* **9**, 3430 (2009).
- ¹⁷D. S. Lee, B. Krauss, L. Patthey, K. von Klitzing, J. H. Smet, U. Starke, C. Coletti, and C. Riedl, *Phys. Rev. B* **81**, 235401 (2010).
- ¹⁸P. C. Rusu, G. Brocks, J. van den Brink, P. J. Kelly, P. A. Khomyakov, and G. Giovannetti, *Phys. Rev. B* **79**, 195425 (2009).
- ¹⁹S. Honda, H. Bente, S. Ito, H. Ohkita, H. Tsuji, A. Orimo, and K. Masuda, *Appl. Phys. Lett.* **96**, 043305 (2010).
- ²⁰Y. Q. Li, M. K. Fung, Z. Xie, S.-T. Lee, L.-S. Hung, and J. Shi, *Adv. Mater. (Weinheim, Ger.)* **14**, 1317 (2002).
- ²¹P. Peumans, A. Yakimov, and S. R. Forrest, *J. Appl. Phys.* **93**, 3693 (2003).
- ²²J. Ho, D. Nezhich-Hyungbin, S. Vladimir, B. Mildred, S. Dresselhaus, A. Reina, X. Jia, and J. Kong, *J. Am. Chem. Soc.* **9**, 30 (2009).
- ²³W. Cai, M. Borysiak-Boyang, H. David, C. Richard, D. Piner, L. Colombo-Rodney, S. Ruoff, X. Li, and Y. Zhu, *ACS Nano* **9**, 4359 (2009).
- ²⁴L. G. De Arco, Y. Zhang, A. Kumar, and C. Zhou, *IEEE Trans. NanoTechnol.* **8**, 135 (2009).
- ²⁵Y. Lee, X. Xu-Jae-Sung, P. Yi, Z. Jayakumar, B. Tian, L.-H. Ri, K. Young, I. Song, Y.-J. Kim, K. S. Kim, B. Ozyilmaz, J.-H. Ahn, B. Hee, H. Sumio, L. S. Bae, and H. Kim, *Nat. Nanotechnol.* **5**, 574 (2010).
- ²⁶Y. Zhong, F. Zhu, Y. Wang, X. Chen, and K. P. Loh, *Appl. Phys. Lett.* **95**, 112902 (2009).